Embedded-atom-method interatomic potentials for hcp metals

R. Pasianot and E. J. Savino

Comisión Nacional de Energía Atómica, Avenida del Libertador 8250, 1429 Buenos Aires, Argentina

We develop here an empirical procedure for constructing embedded-atom-method (EAM) interatomic potentials for hcp metals. This is based on fitting perfect-crystal lattice properties. The contribution of the lattice inner degrees of freedom, due to the two atoms per lattice site, is included into the elastic response of the crystal. It is found that the elastic constants of several hcp pure metals cannot be fitted within the EAM. For example, no valid potential can be constructed for Cd, Zn, Be, and Y, which properly adjust the measured elastic constants. Neither could we find an appropriate fit for Zr.

I. INTRODUCTION

Many-body interatomic potentials either called embedded-atom-method (EAM)[1] or empirical many-body potential[2] [Finnis and Sinclair (FS)] have been applied successfully to the simulation of a variety of defects, mainly in fcc- and bcc-related structures.[3] Within that approach, the total energy may be written as

$$E = \sum_i E_i \, , \tag{1}$$

where the contribution from the atom at site i is

$$E_i = \tfrac{1}{2} \sum_{j \, (\neq i)} V(R_{ij}) + F(\rho_i) \, , \tag{2}$$

j points to a neighbor atom located at the position $\mathbf{R}_{ij}$ with the origin at i, $V(R)$ is a standard pair-interaction term and $F(\rho)$ is the so-called "embedding function." ρ stands for the "local electronic density" and is given as a superposition of pair functions:

$$\rho_i = \sum_{j \, (\neq i)} \phi(R_{ij}) \, . \tag{3}$$

Although not generally done by other authors, in Eq. (2) it is convenient to impose the many-body term F to have null first derivative at the perfect lattice density. This gauge, used hereafter, defines $V(R)$ as an effective pair-interaction potential.[2] This pair potential should predict a homogeneously stressed lattice under the appropriate Cauchy pressure with the correct lattice parameter. Local many-body terms should therefore mainly affect the relaxation pattern in the neighborhood of a defect and they may be considered as higher-order terms in a series expansion of the lattice energy.

Compared to the pair potentials, the above potentials give a more realistic picture of static configurations and dynamics of lattice defects, while the calculation remains within reasonable computing times.[3]

Contrary to the cubic structures, the hcp structure has not been extensively studied using these kind of potentials. Oh and Johnson[4] developed in 1988 empirical many-body interaction potentials for Mg, Ti, and Zr; Willaime and Massobrio[5] did so for Zr and Igarashi,

Kanta, and Vitek (IKV)[6] developed relatively more realistic interatomic potentials for Zn, Mg, Be, Co, Zr, Ti, Ru, and Hf. All those works neglect the contribution of the lattice inner degrees of freedom to the elastic constants. This is null for centrosymmetric lattices[7] and IKV[6] claim this contribution is not important in their case. However, it was already noticed[8] that disregarding this internal relaxation led to an important miscalculation of the C_{44} shear in Si. Therefore, it may be relevant to hcp crystals.

In Sec. II next, we deduce the elastic constants for an hcp lattice in terms of the interatomic potential derivatives. We find that not all sets of experimental elastic constants can be fitted within the EAM. In Sec. III, a scheme is developed for building the potentials and subsequently applied to several hcp metals. Finally, and in the light of our previous work,[9] we discuss briefly the possibility of improving the EAM in order to fit the measured elastic constants of any hcp metal.

II. ELASTIC CONSTANTS FOR hcp CRYSTALS

In 1965 Czachor[10] deduced the elastic constants for hcp crystals in terms of the components of the dynamical matrix. Later, the expression for those constants was obtained in the case of a pair interatomic potential with a third-neighbors interaction range.[11] Both works rely on the method of long waves,[7] where the elastic constants are obtained as a by-product of the dynamical matrix in the long-wave length limit. More recently, Martin[12,13] has given a thorough analysis of the method of uniform deformation applied to general monoatomic lattices; this author writes the energy density as an expansion in atomic clusters of arbitrary order. We use here an extension of the method of uniform deformation applied to the hcp lattice, as it was done before for the cubic metals,[9] assuming an interaction of the EAM type. This allows full use of symmetry properties, resulting in a relatively simple algebraic manipulation. In brief, a uniform strain is applied to the crystal and the energy change is evaluated. The latter quantity is given as a quadratic form (positively defined) of the strain components. To calculate the coefficients of the energy expansion, which are directly related to the elastic constants, a convenient tensor basis is employed.

If a virtual displacement $d\mathbf{R}_{ij}$ of the j neighbor of site i is imposed, the EAM energy of Eq. (2) can be expanded to second order as

$$dE_i = \tfrac{1}{2}\sum_j V'(R_{ij})dR_j + \tfrac{1}{4}\sum_j V_j''(R_{ij})(dR_j)^2 + \tfrac{1}{2}F_0''(\delta\rho_i)^2 ,$$

(4a)

where

$$dR_j = \langle \mathbf{r}_{ij}|d\mathbf{R}_{ij}\rangle + 1/(2R_{ij})\langle\overset{\leftrightarrow}{\delta} - \mathbf{r}_{ij}\otimes\mathbf{r}_{ij}|d\mathbf{R}_{ij}\otimes d\mathbf{R}_{ij}\rangle$$

(4b)

and

$$\delta\rho_i = \sum_j \phi'(R_{ij})dR_j = \sum_v \phi_v' \sum_{j\in v} dR_j .$$

(4c)

$\mathbf{r}_{ij}$ is a unit vector pointing from atom i to j, the symbols f' and f'' stand, respectively, for first and second derivatives of the function f, whereas ($\mathbf{A}\otimes\mathbf{B}$) is the dyadic tensor:

$$(\mathbf{A}\otimes\mathbf{B})_{\alpha\beta} = A_\alpha B_\beta .$$

$\langle\mathbf{A}|\mathbf{B}\rangle$ is shorthand for the scalar product

$$\langle\mathbf{A}|\mathbf{B}\rangle = \sum_{\alpha,\beta,\ldots} A_{\alpha\beta}\ldots B_{\alpha\beta}\ldots ,$$

and $\overset{\leftrightarrow}{\delta}$ is the Kronecker tensor of rank 2.

In (4c) the sum over j was decomposed as a sum over the atomic shells that surround the reference site; this simplifies the algebra because each shell retains the lattice symmetry.

When a uniform strain is applied to an hcp crystal, the lack of inversion symmetry with respect to the atomic positions imposes forces between the two Bravais lattices of the hcp structure. These forces are relaxed in order to minimize the elastic energy.[7] This (virtual) elastic energy not only depends on the square of the strain components, but also on the relative displacement of the two lattices ("internal strains"). Therefore, under a homogeneous strain $\overset{\leftrightarrow}{\epsilon}$ the atomic positions change by

$$d\mathbf{R}_{0j} = \begin{cases} \overset{\leftrightarrow}{\epsilon}\cdot\mathbf{R}_{0j}, & \text{if } j\subset\mathcal{L}_0 , \\ \overset{\leftrightarrow}{\epsilon}\cdot\mathbf{R}_{0j} + \mathbf{s}, & \text{if } j\not\subset\mathcal{L}_0 , \end{cases}$$

(5a)

(5b)

where $j\subset\mathcal{L}_0$ stands for the atomic positions of the same sublattice than the reference origin 0, $j\not\subset\mathcal{L}_0$ for the other sublattice, and $\mathbf{s}$ is the displacement between the two of them. The reasoning would be identical if the equicenter between the two lattices were considered:

$$d\mathbf{R}_{0j} = \begin{cases} \overset{\leftrightarrow}{\epsilon}\cdot\mathbf{R}_{0j} - \mathbf{s}/2, & \text{if } j\subset\mathcal{L}_0 , \\ \overset{\leftrightarrow}{\epsilon}\cdot\mathbf{R}_{0j} + \mathbf{s}/2, & \text{if } j\not\subset\mathcal{L}_0 . \end{cases}$$

Replacing (5) into (4a) leads to

$$dE = L(\overset{\leftrightarrow}{\epsilon},\mathbf{s}) + q_1(\overset{\leftrightarrow}{\epsilon}) + q_2(\overset{\leftrightarrow}{\epsilon},\mathbf{s}) + q_3(\mathbf{s}) ,$$

(6)

where $L(\overset{\leftrightarrow}{\epsilon},\mathbf{s})$ is a term linear in $\overset{\leftrightarrow}{\epsilon}$ and $\mathbf{s}$, while the terms q are quadratic in their arguments. Therefore, for a stress-free and force-free lattice, $L(\overset{\leftrightarrow}{\epsilon},\mathbf{s})$ must be zero. The force-free requirement is satisfied as a consequence of the

lattice symmetry. On the other side, the stress-free requirement gives the two equations known as Huang conditions:

$$\sum_v N_v R_v V_v' r_\parallel^2(v) = 0 ,$$

(7a)

$$\sum_v N_v R_v V_v' r_\perp^2(v) = 0 ,$$

(7b)

where v stands for the vth shell about the origin and N_v for the number of atoms belonging to this shell. The decomposition of a vector in parallel and perpendicular components to the axis c was used, namely,

$$\mathbf{r} = \mathbf{r}_\parallel + \mathbf{r}_\perp$$

with

$$r_\parallel = r_3 \quad\text{and}\quad r_\perp = \sqrt{r_1^2 + r_2^2} ,$$

where subindexes 1,2,3 refer to the coordinate axes of Fig. 1. The quadratic terms in the energy expansion, Eq. (6), allow us to deduce the expressions for the elastic constants. On one side, $q_1(\overset{\leftrightarrow}{\epsilon})$ does not depend on the relative displacement between sublattices and it is, therefore, the quadratic contribution to the energy for a simple hexagonal lattice which agrees with the expressions deduced in Refs. 4 and 6, where inner degrees of freedom were not considered. On the other, $q_2(\overset{\leftrightarrow}{\epsilon},\mathbf{s})$ contains the coupling terms, cross-products between displacements and strains. Finally, $q_3(\mathbf{s})$ is a function only of the relative displacement.

In the coordinate system sketched in Fig. 1 we find after some little algebraic manipulations:

$$q_2(\overset{\leftrightarrow}{\epsilon},\mathbf{s}) = [(\epsilon_{11} - \epsilon_{22})s_1 - 2s_2\epsilon_{12}]P/4 ,$$

(8)

$$q_3(\mathbf{s}) = s_\parallel^2 Q_\parallel/4 + s_\perp^2 Q_\perp/4 ,$$

(9)

where

$$P = {\sum_v}' \tfrac{1}{2}N_v(V_v'' - V_v'/R_v)R_v r_\perp^3(v)\cos(3\alpha_v) ,$$

(10)

$$Q_\parallel = {\sum_v}' N_v[V_v'' + r_\perp^2(v)(V_v'/R_v - V_v'')] ,$$

(11)

$$Q_\perp = {\sum_v}' N_v[V_v'/R_v + \tfrac{1}{2}r_\perp^2(v)(V_v'' - V_v'/R_v)] .$$

(12)

The sums of (10), (11), and (12) extend over the atomic shells that do not belong to the same sublattice than the
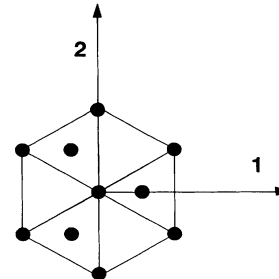

FIG. 1. Sketch of the (0001) stacking in the hcp structure showing the reference coordinate axes used.

reference atom (the sum in this case is indicated with $\sum'$) and α_ν is the angle between $\mathbf{r}_\perp$ and the positive sense of axis 1 (see Fig. 1). (Note that axis 1 belongs to a vertical mirror plane.) With $L(\overline{\epsilon}, \mathbf{s}) = 0$, the minimum of Eq. (6) with respect to the displacements gives

$$\partial E / \partial s_\parallel = 0 \Longrightarrow s_\parallel = 0 , \tag{13a}$$

$$\partial E / \partial s_1 = P(\epsilon_{11} - \epsilon_{22}) + 2s_1 Q_\perp \tag{13b}$$

$$= 0 \Longrightarrow s_1 = -P/2Q_\perp(\epsilon_{11} - \epsilon_{22}) ,$$

$$\partial E / \partial s_2 = -2P\epsilon_{12} + 2s_2 Q_\perp = 0 \Longrightarrow s_2 = P/Q_\perp \epsilon_{12} . \tag{13c}$$

Therefore, Eq. (6) can be rewritten as

$$dE = q_1(\overline{\epsilon}) - \tfrac{1}{2}(P^2/4Q_\perp)[(\epsilon_{11} - \epsilon_{22})^2/2 + 2\epsilon_{12}^2] . \tag{14}$$

By lattice symmetry arguments and proper mathematical handling, it can be seen that the second term of Eq. (14) contributes only to the $(c_{11} - c_{12})$ eigenvalue of the Voigt matrix.

Finally, the following equations for the five independent elastic constants of an hcp crystal are obtained:

$$F_0'' \sum (r_\parallel)^2 \sum (r_\perp)^2 = 2\Omega(c_{13} - c_{44}) , \tag{15a}$$

$$\sum_\nu N_\nu r_\parallel^4(\nu)\psi_\nu = 2\Omega c_{33} - 4\Omega(c_{13} - c_{44}) \sum (r_\parallel)^2 \Big/ \sum (r_\parallel)^2 , \tag{15b}$$

$$\sum_\nu N_\nu r_\perp^4(\nu)\psi_\nu$$
$$= 4\Omega(c_{11} + c_{12}) - 4\Omega(c_{13} - c_{44}) \sum (r_\perp)^2 \Big/ \sum (r_\parallel)^2 , \tag{15c}$$

$$\sum_\nu N_\nu r_\perp^2(\nu) r_\parallel^2(\nu)\psi_\nu = 4\Omega c_{44} , \tag{15d}$$

$$(1/\Omega)(P^2/4Q_\perp)$$
$$= \tfrac{1}{2}(3c_{12} - c_{11}) - \tfrac{1}{2}(c_{13} - c_{44}) \sum (r_\perp)^2 \Big/ \sum (r_\parallel)^2 , \tag{15e}$$

where Ω is the atomic volume and

$$\sum (r_\perp)^2 = \sum_\nu N_\nu R_\nu \phi_\nu' r_\perp^2(\nu) ,$$

$$\sum (r_\parallel)^2 = \sum_\nu N_\nu R_\nu \phi_\nu' r_\parallel^2(\nu) ,$$

$$\psi_\nu = R_\nu^2 V_\nu'' - R_\nu V_\nu' .$$

As $Q_\perp$ is the coefficient of s_1^2 in the quadratic positively defined expression, Eq. (6) [and therefore Eq. (9)], the left-hand side of Eq. (15e) happens to be positive, implying a restriction on the potential fit. Also, if ϕ is a monotonous decreasing function[1,2] the sign of the right-hand side of Eq. (15e) is nearly independent of the particular functional form of ϕ. For geometrical reasons

$$\sum (r_\perp)^2 \Big/ \sum (r_\parallel)^2 \simeq 2 . \tag{16}$$

Therefore, the EAM model imposes the following restriction on the elastic constants of an hcp structure:

TABLE I. Experimental values for the two members of Eq. (17a) C_{ij} in eV/Å^3, values taken from Ref. 23.

	$(3C_{12} - C_{11})/2$	$(C_{13} - C_{44})$	c/a
Be	−0.67	−0.97	1.568
Y	0.012	−0.05	1.572
Hf	0.11	0.037	1.581
Ti	0.26	0.11	1.588
Zr	0.14	0.18	1.593
Sc	0.09	0.01	1.594
Tl	0.22	0.13	1.598
Mg	0.047	0.025	1.624
Co	0.55	0.12	1.623
Zn	−0.20	0.06	1.856
Cd	−0.028	0.106	1.886

$$\tfrac{1}{2}(3c_{12} - c_{11}) > c_{13} - c_{44} . \tag{17a}$$

Table I summarizes the experimental values of the two members of Eq. (17a) for several hcp metals. It can be seen that no EAM interatomic potential can be fitted to the elastic constants of Zn and Cd, whereas Zr is a doubtful case depending mainly on the number of neighboring shells included within the range of ϕ. Our fitting scheme developed in Sec. III is unable to give a potential for Zr. This explains the observations of IKV[6] regarding the somewhat unphysical behavior observed in their potentials for Zn and Zr, and the impossibility to fit a potential for Cd.

On another hand, Eq. (15a) shows that the sign of F'' at the equilibrium density (F_0'') is determined, within the EAM, by $(c_{13} - c_{44})$. A negative F_0'' implies that the many-body part of the energy would tend to destabilize the lattice structure. This same argument is developed by Daw[14] and from a more fundamental side the need of a positive F_0'' is clearly explained by Carlsson.[15] Therefore, in addition to (17a) an EAM potential can be fitted to the elastic constants, provided

$$c_{13} - c_{44} > 0 \tag{17b}$$

which is not the case for Be and Y, see Table I.

III. INTERATOMIC POTENTIAL FITTING

In this section we develop a procedure to obtain an EAM interatomic potential for the hcp metals. This is built to match the lattice parameters a and c, the cohesive energy, the vacancy formation energy, and the elastic constants, Eqs. (15). The potentials are developed only for metals where those constants satisfy the condition of Eqs. (17a) and (17b). The independent fitting of a and c is obtained by fulfilling the two equations (7) (Huang conditions). From Eq. (2) the cohesive energy of the crystal at equilibrium is

$$E_c = -\left[\tfrac{1}{2} \sum_\nu N_\nu V_\nu + F_0 \right] . \tag{18}$$

In addition, for extending the validity of the potential outside the near equilibrium configurations, the expres-

TABLE II. Data fitted by the potentials. (a) The basal lattice parameter a and c/a ratio are from Ref. 24. Cohesive energies E_c from Ref. 25. The vacancy formation energy E_f^v is $\frac{1}{3} E_c$ for Hf and Co, whereas for Mg it is from Ref. 27 and for Ti from Ref. 26. (b) Elastic constants C_{ij} in eV/Å^3 from Ref. 23.

| | (a) | | | |
	a (Å)	c/a	E_c (eV)	E_f^v (eV)
Hf	3.194	1.581	6.44	2.15
Ti	2.951	1.588	4.85	1.55
Mg	3.209	1.624	1.51	0.80
Co	2.507	1.623	4.39	1.46

| | (b) | | | | |
	C_{11}	C_{33}	C_{44}	C_{12}	C_{13}
Hf	1.1866	1.2759	0.3745	0.4650	0.4089
Ti	1.0992	1.1891	0.3171	0.5424	0.4263
Mg	0.3962	0.4148	0.1150	0.1619	0.1355
Co	1.9944	2.3321	0.5144	1.0368	0.6373

sion of Rose et $al.$[16] is used. Those authors propose a universal dependence of the cohesive energy on the lattice parameter:

$$E(\bar{a}) = -E_c(1+\bar{a})e^{-\bar{a}} \qquad (19)$$

with

$$\bar{a} = 3[(\Omega\langle B \rangle)/E_c]^{1/2}(a/a_0 - 1)$$

and

$$\langle B \rangle = \frac{1}{9}(2c_{11} + 2c_{12} + 4c_{13} + c_{33}) ,$$

where a is the basal lattice parameter and a_0 the equilibrium parameter. $\langle B \rangle$ is the average (Voigt) bulk modulus, and its definition is consistent with the elastic response to uniform dilations implied by Eqs. (15).

Finally, the vacancy formation energy can be fitted. Without allowing for lattice relaxation, this energy re-

sults:[9]

$$E_f^v = -\frac{1}{2} \sum_v N_v V_v + \frac{1}{2}F_0'' \sum_v N_v \phi_v^2 . \qquad (20)$$

For fitting the potential, first a functional form for the electronic potential $\phi(r)$ must be assumed. Afterward, Eqs. (7), (15), (18), (19), and (20) constitute a set of nine equations with F_0, F_0'', and the pair-potential parameters as unknowns.

As an electronic potential we choose a Thomas-Fermi screening function

$$\phi(r) = e^{-\beta r/a}/(r/a) \quad \text{with} \quad \beta = 5 \qquad (21)$$

as we already did in a previous work,[9] smoothly matched to zero at $r/a = 2.1$.

For the pair interaction we choose a seven-piece cubic polynomial, continuous at the matching nodes together

TABLE III. Potential parameters R_i in units of a, A_i, F_0, and F_0'' in eV.

	Hf	Ti	Mg	Co
R_1	2.1	2.1	1.8	2.1
R_2	1.8	1.8	1.75	1.8
R_3	1.7	1.7	1.73	1.7
R_4	1.65	1.65	1.72	1.5
R_5	1.4	1.4	1.4	1.3
R_6	1.02	1.05	1.05	1.1
R_7	1.0	1.0	1.0	1.0
A_1	0.540 962 53	0.426 267 08	$-5.126 962 16$	0.263 789 17
A_2	$-4.934 796 2$	$-2.460 913 26$	15.965 471 7	$-0.707 060 79$
A_3	$-9.759 854 4$	$-7.168 303 10$	$-31.000 515 6$	$-1.801 508 45$
A_4	18.344 396 3	10.631 178 6	21.084 575 0	2.698 423 62
A_5	$-3.728 852 8$	$-0.807 124 1$	$-0.312 737 49$	$-0.350 486 95$
A_6	197.905 819 2	50.249 469 0	23.329 048 4	32.524 020 0
A_7	$-199.888 792$	$-42.260 581 6$	$-24.147 421 8$	$-4.109 211 22$
F_0	-4.296	-3.316	-0.714	-2.941
F_0''	20.430	52.286	14.132	40.271

with the first and second derivatives:[17]

$$V(r) = \sum_{k=1}^{7} A_k (R_k - r)^3 H(R_k - r) ,\qquad (22)$$

where $H(x)$ is the Heaviside function

$$H(x) = \begin{cases} 0, & \text{if } x \leq 0 , \\ 1, & \text{if } x > 0 . \end{cases}$$

The seven coefficients of Eq. (22) constitute the remaining unknowns of the set of equations mentioned above. The positions of the matching nodes (and particularly the cut-off distance) can be properly selected to obtain a stable hcp structure against other crystal lattices and reasonable values for the stacking fault energies. The system of equations is well stated and easily solved, despite the nonlinearity implied in (15e). It may be viewed as finding the intersection points of a straight line in N-dimensions, determined by all the equations but (15e),
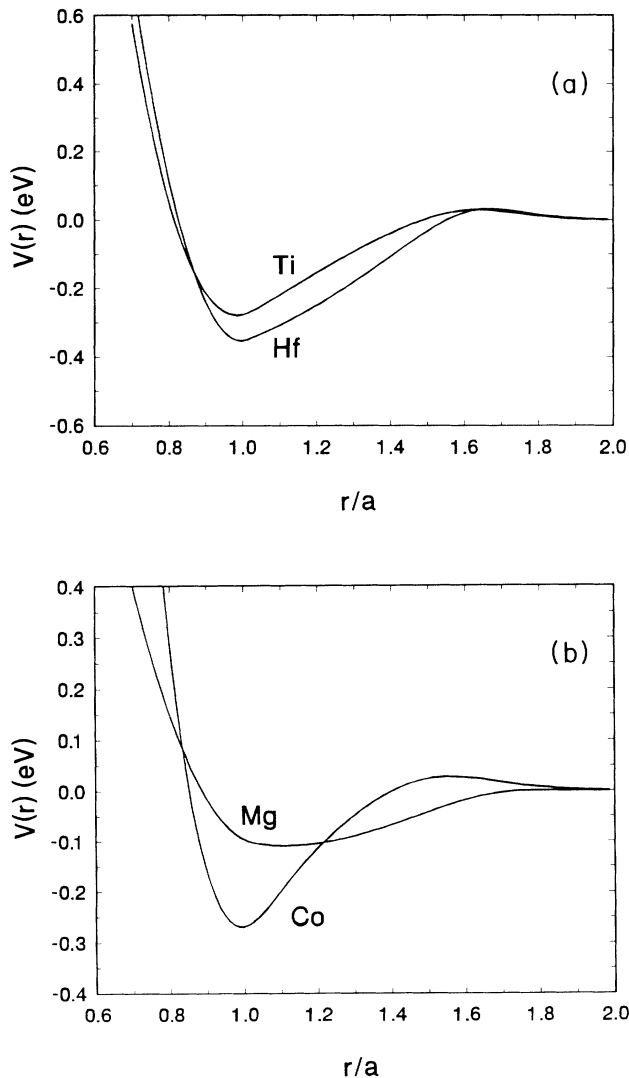
and a quadratic surface defined by (15e).

To obtain the embedding function $F(\rho)$ consistent with the deduced values of F_0 and F_0'', Eqs. (2) and (19) are used, i.e., a numerical fit of $F(\rho)$ to Eq. (19) and the above expressions for the density and pair part of the interaction is done.[18]

The method outlined above is applied to the metals Mg, Co, Ti, and Hf. The experimental data used is summarized in Table II, and the parameters defining the effective pair potential of Eq. (22) are given in Table III. The latter function is also plotted in Fig. 2.

IV. DISCUSSION AND CONCLUSIONS

We have obtained many-body EAM interatomic potentials for Hf, Ti, Mg, and Co. Those potentials fit the lattice parameters in equilibrium, cohesive energy (including its dependence with pressure), vacancy formation energy, and elastic constants.

In addition, we showed in Sec. III that the EAM does not allow us to obtain an appropriate fitting to the elastic constants of Be, Y, Zn, and Cd and, for reasons there discussed, we have not been able to do so for Zr.

The EAM potentials deduced above should predict a stable hcp lattice against other possible structures and reasonable values for the energy of extended defects. We have checked their stability against the fcc phase and calculated the I_2 stacking fault energy on the basal plane, which must be positive. These quantities are reported in Table IV. As it is expected, both quantities, i.e., the energy difference with the fcc phase and the stacking fault energy, are strongly correlated. Within the fitting procedure both energies were optimized by varying the knot positions of the pair potential and at the same time trying to obtain a "well-behaved" function. However, the values for the stacking fault energy so obtained are at best reasonable. The situation regarding this point is controversial, there is no general agreement between experimentally reported values[19-21] and theoretically calculated ones.[22] Nonetheless, the authors' feeling is that the obtained values are probably too small, particularly for Ti and Hf, as results from comparison with values reported by Legrand.[22] We also found that the many-body contribution to the stacking fault energy is of minor importance. For example, in order to get a positive value the effective pair potential must have an interaction range beyond fourth neighbors of the hcp structure. This is the same situation encountered with simple pair potentials.

Regarding previous work done in hcp metals, we believe that ours has some advantages. The work of Oh

FIG. 2. Effective pair potentials for Ti and Hf (a), and Co and Mg (b).

TABLE IV. Calculated properties: ΔE is the energy difference with a metastable fcc phase; γ is the I_2 stacking fault energy.

	ΔE (eV/atom)	γ (mJ/m^2)
Hf	0.039	154
Ti	0.023	104
Mg	0.0083	30
Co	0.007	41

and Johnson[4] only adjusts two average elastic constants and adopts fully empirical expressions for the potential shape. Willaime and Massobrio[5] try a more physically solid approach to the potential analytic expressions based on tight-binding approximations. This allows them to include the phase transformation in Zr. However, these authors do not attempt a proper fitting to the elastic constants in either phase (bcc and hcp). Finally, IKV[6] do a more careful empirical fit of their potential. We shall concentrate hereafter in comparing our results with those of IKV.

It is interesting to compare our system of equations to fit EAM potentials to hcp metals with the one used by IKV. Apart from our gauging that makes of the pair part an effective potential, the main difference appears to be (1) that IKV do not adjust any pressure dependence of the cohesive energy and (2) the different fitting of the elastic constants.

To adjust a pressure dependence of the cohesive energy may be very important for large density clusters; for example, at the neighborhood of an interstitial atom. Therefore, for the case of cubic structure metals it is common practice[18] to fit the EAM potential to Rose et al.[16] expression as done by us above. However, a nonfortunate selection of the fitting polynomial functions for the pair part of the interactions may cause a change in the curvature for distances below first neighbors. This is the cause of the difference between the FS[2] potential for Nb and ours as compared in Ref. 9. Therefore, we have either tried to avoid this change or tried its occurrence at distances very near the origin in the hope those distances would not be reached in the applications.

Regarding the equations for the elastic constants, IKV instead of fitting the many-body part of the potential to the Cauchy pressure term $(c_{13}-c_{44})$, Eq. (15a), as we do, they adjust the value of $c_{12}-c_{66}=(3c_{12}-c_{11})/2$. Their Eq. (7) for this elastic constant is obtained by combining our Eqs. (15a) and (15e) if P^2 is set to zero. This implies that, as said above, IKV's potentials are not in equilibrium for the internal degrees of freedom of the lattice, i.e., do not satisfy Eq. (15e). The contribution of the inner strains may be even larger than the many-body contribu-

tion, as is clearly evidenced in Table V. In the first column of Table V the experimental values of $(c_{12}-c_{66})$ are reported (remember that this is the elastic constant that the many-body term of IKV tries to fit). The relative importance of the inner degree of freedom, neglected by IKV, is reflected in the values of $P^2/4Q_1$ of Eq. (15e). This quantity, calculated by using IKV's potentials and ours are, respectively, reported in the second and third columns of Table V. It appears that the worst cases, those where neglecting inner strains implies a large error, are Hf, Ru, and Zr. For Ti and Mg the inner strains contribution only amounts to, respectively, 10 and 20 % of the value of $(3c_{12}-c_{11})/2$, see Eq. (15e) and Table V. Therefore in these cases, IKV's potentials should be similar to ours and some of the differences observed in Fig. 3 may be due to a difference in the fitting procedure.

Any discrepancy in fitting the elastic constants should show in the slope at the origin of the phonon dispersion
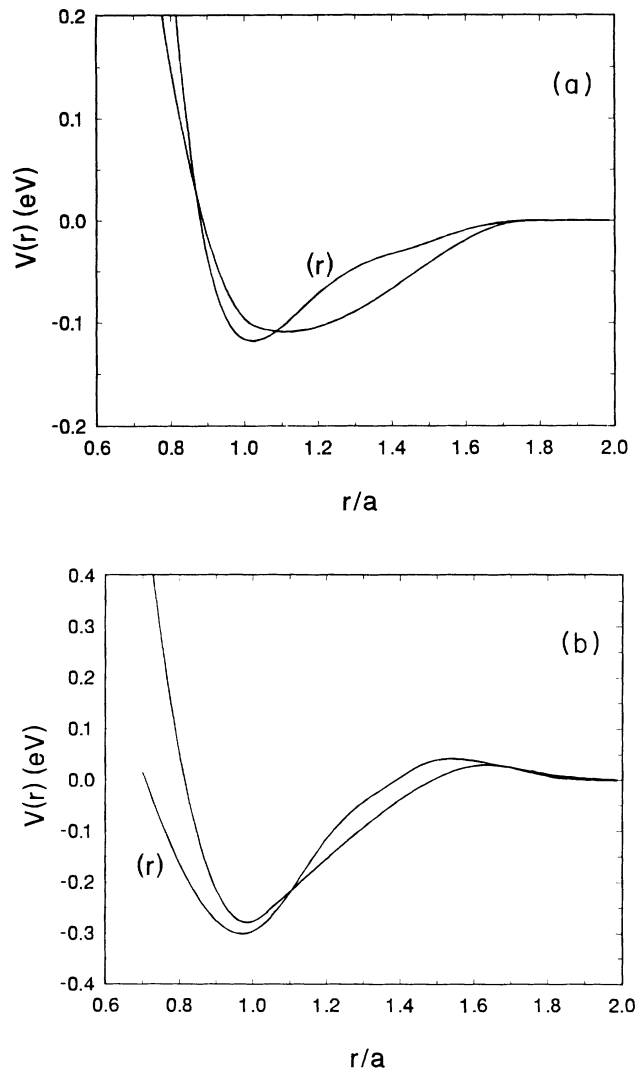

FIG. 3. Comparison between effective pair potentials for Mg (a) and Ti (b). The curve without a label is from this work whereas (r) is from Ref. 6.

TABLE V. Inner strains contribution $P^2/4Q_1$ for several hcp metals in eV.

Metal	$(C_{12}-C_{66})\Omega$[a]	$P^2/4Q_1$[b]	$P^2/4Q_1$[c]
Hf	2.324	5.207	1.596
Ti	4.665	0.578	2.823
Mg	1.040	0.225	0.571
Co	6.179	0.901	4.842
Be[e]	−5.482	2.152	
Ru[e]	−0.655[d]	6.736	
Zr[e]	3.360	5.120	
Zn[e]	−3.161	2.192	

[a]Experimental values.
[b]Calculated from Ref. 6.
[c]This work.
[d]Low temperature value.
[e]No EAM interatomic potential fitting was attempted by us.

curves. Due to scaling reasons this point is difficult to clarify from IKV's plots, however, inconsistencies are apparent in some cases. For example, the slope shown in their Fig. (6b) for the calculated transversal acoustic [100] branches for Hf differs from the experimental one. The measured values of c_{44} and c_{66} are 0.37 and 0.36 eV/$\mathring{A}^3$, respectively, and both branches should nearly coincide at $k = 0$, as experimentally evidenced. The fact is that IKV's calculation of the phonon spectra is the correct one for the interatomic potential adopted; while their expression for fitting the elastic constants, does not include the internal strains that necessarily appear in an elastically distorted lattice held by the same potential.

Finally, in Ref. 9 we found that, for fitting some of the properties of Cr, a bcc transition metal, the inclusion of an angle-dependent term in the many-body part of the cohesive energy was needed. Here we have seen that the EAM is not suitable for several hcp metals. We are developing therefore an approach analogous to the one of Ref. 9, in the hope this might solve the above drawback of the EAM when applied to hcp transition metals.

[1] M. S. Daw and M. I. Baskes, Phys. Rev. B **29**, 6443 (1984).

[2] M. W. Finis and J. E. Sinclair, Philos. Mag. A **50**, 45 (1984).

[3] V. Vitek and D. J. Srolovitz, editors, *Atomistic Simulation of Materials* (Plenum, New York, 1989).

[4] D. J. Oh and R. A Johnson, J. Mater. Res. **3**, 471 (1988).

[5] F. Willaime and C. Massobrio, Phys. Rev. B **43**, 11 643 (1991).

[6] M. Igarashi, K. Kanta, and V. Vitek, Philos. Mag. B **63**, 603 (1991).

[7] M. Born and K. Huang, *Dynamical Theory of Crystal Lattices* (Clarendon, Oxford, 1956).

[8] M. I. Baskes, J. S. Nelson, and A. F. Wright, Phys. Rev. B **40**, 6085 (1989).

[9] R. Pasianot, D. Farkas, and E. J. Savino, Phys. Rev. B **43**, 6952 (1991).

[10] A. Czachor, in *Inelastic Scattering of Neutrons* (IAEA, Vienna, 1965), Vol. I, p. 181.

[11] A. J. Trott and P. T. Heald, Phys. Status Solidi B **46**, 361 (1971).

[12] J. W. Martin, J. Phys. C **8**, 2837 (1975).

[13] J. W. Martin, J. Phys. C **8**, 2869 (1975).

[14] M. S. Daw, in *Atomistic Simulation of Materials* (Ref. 3), p. 181.

[15] A. E. Carlsson, in *Solid State Physics* **43**, 1 (1990).

[16] J. H. Rose, J. R. Smith, F. Guinea, and J. Ferrante, Phys. Rev. B **29**, 2963 (1984).

[17] G. J. Ackland, G. Tichy, V. Vitek, and M. W. Finnis, Philos. Mag. A **56**, 735 (1987).

[18] S. M. Foiles, M. I. Baskes, and M. S. Daw, Phys. Rev. B **33**, 7983 (1986).

[19] P. Partridge, Metall. Rev. **118**, 169 (1967).

[20] H. P. Leighly, Philos. Mag. **22**, 209 (1970).

[21] R. E. Smallman and P. S. Dobson, Metall. Trans. **1**, 2328 (1970).

[22] B. Legrand, Philos. Mag. B **49**, 171 (1984).

[23] G. Simmons and H. Wang, *Single Crystal Elastic Constants and Calculated Aggregate Properties: A Handbook* (MIT Press, Cambridge, Massachusetts, 1971).

[24] W. B. Pearson, *A Handbook of Lattice Spacings and Structure of Metals and Alloys* (Pergamon, Oxford, England, 1958), Vols. 1 and 2 (1967).

[25] C. Kittel, *Introduction to Solid State Physics* (Wiley Interscience, New York, 1986).

[26] V. O. Shestopal, Fiz. Tverd. Tela (Leningrad) **7**, 3461 (1966) [Sov. Phys. Solid State **7**, 2798 (1966)].

[27] C. Mairy, J. Hillairet, and D. Schumacher, Acta Metall. **15**, 1258 (1967).